Preprint
UCRL-JC-140458

# Quantitative Estimation of Trace Chemicals in Industrial Effluents with the Sticklet Transform Method

*N. C. Mehta, E. T. Scharlemann, C. G. Stevens*

This article was submitted to
Chemical and Biological Sensing II
Orlando, FL
April 16-20, 2001

**April 2, 2001**

*U.S. Department of Energy*

Lawrence
Livermore
National
Laboratory

# Quantitative Estimation of Trace Chemicals in Industrial Effluents with the Sticklet Transform Method

Naresh C. Mehta[1], E. T. Scharlemann, Charles G. Stevens
Lawrence Livermore National Laboratory, L-183
Livermore, CA 94550

## ABSTRACT

Application of a novel transform operator, the Sticklet transform, to the quantitative estimation of trace chemicals in industrial effluent plumes is reported. The sticklet transform is a superset of the well-known derivative operator and the Haar wavelet, and is characterized by independently adjustable lobe width and separation. Computer simulations demonstrate that we can make accurate and robust concentration estimates of multiple chemical species in industrial effluent plumes in the presence of strong clutter background, interferent chemicals and random noise. In this paper we address the application of the sticklet transform in estimating chemical concentrations in effluent plumes in the presence of atmospheric transmission effects. We show that this transform retains the ability to yield accurate estimates using on-plume / off-plume measurements that represent atmospheric differentials up to 10 % of the full atmospheric attenuation.

*Key words:* Sticklet transform, Haar wavelets, derivative spectroscopy, classical least squares, remote chemical sensing, concentration estimation.

## 1. INTRODUCTION

The measurement of chemical effluents by remote airborne, or even space-based, ultra-spectral infrared spectrometry presents an attractive technological approach to wide area chemical monitoring. However, before this technology can be implemented as a quantitative tool, the problem of separating gaseous target signatures from background spectral features must be solved. A number of approaches to this problem are under active investigation. The most popular among these take advantage of the extensive information provided by imaging spectrometers. The techniques of principal component analysis[1] and matched filtering[2] use this information to identify spectral components in the background surrounding the plume. The quality of the results rests on the assumption that the materials under the plume are to be found in the surrounding scene; at some level this assumption breaks down. In order to mitigate this constraint, techniques that do not rely on the similarity of this background need to be developed.

Derivative spectroscopy is a popular tool among analytical chemists due to its ability to detect weak absorption features in the vicinity of strong lines. But its usefulness can be limited by its susceptibility to high-frequency random noise. In feature extraction studies using wavelets[3,4], components of varying sizes and strengths, superimposed on a broad background, have been detected with wavelets of different scales. To the best of our knowledge, however, no study has reported a quantitative estimation of component strengths in cluttered signals using wavelet analysis.

We recently reported[5] a novel method of feature extraction from cluttered signals. We employed wavelet-like transform operators, called Sticklets, in the detection and concentration estimation of chemical species in atmospheric remote sensing data at optical wavelengths. We demonstrated the superior performance of the sticklet transform in robust estimation of trace chemical concentrations against a wide variety of backgrounds in clutter-dominated remote sensing scenarios. We studied the susceptibility of the sticklet transform estimation in the presence of random noise and ambient chemical interferents, and investigated effects of sensor binning and instrument lineshape. A comparison showed the sticklet transform method to be superior to derivative and Haar

[1]Contact author: mehta7@llnl.gov

wavelet operators in concentration estimation. It was recognized that atmospheric transmission would pose a significant hurdle because of the presence of a large number of sharp absorption lines of atmospheric constituents in the mid-IR spectral band.

In this report, we investigate the impact of atmospheric transmission at mid-IR wavelengths on the performance of the sticklet method. We begin with an exposition of sticklets in the next section, describing their properties, and contrasting them with wavelets and derivative operators. We then present results of computer simulations to demonstrate the superior predictive capability of sticklets in multivariate feature extraction compared to the classical least squares method. Simulation results including atmospheric transmission effects follow, ending with a few concluding remarks.

## 2. STICKLET TRANSFORM

One of the simplest waveforms used in wavelet analysis[6-10] is the Haar wavelet, which comprises two adjacent lobes with equal widths and equal but opposite amplitudes; the separation between the two lobe centers equals the lobe width. An extension of the Haar wavelet is the concept of a Sticklet operator where the two lobes are separated, i.e. a sticklet has a stick-figure resemblance to a Haar wavelet. One can generate a family of sticklet operators by independently adjusting their lobe widths and separations; Figure 1 illustrates the triangular sticklet space encompassed by sticklets of varying lobe widths and separations. One immediately realizes from Figure 1 that Haar wavelets form a subset of sticklets.

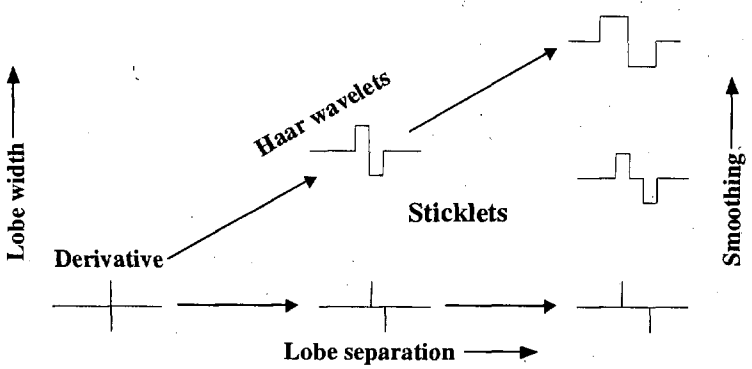


Figure 1. Stcklet space spanned by lobe separation along the abscissa and lobe width along the ordinate. Haar wavelets scale along the diagonal. Smoothing of sticklets occurs as one moves vertically up from the $x$-axis.

In the lower left-hand corner of Figure 1, we have the derivative operator with both lobe width and separation of one bin. Starting with the derivative operator, as one moves along the diagonal, one encounters Haar wavelets at larger scales, with lobe widths and separations increasing together. Similarly, we can define sticklets along the abscissa that are characterized by lobe width of one bin but increasing lobe separation. From any point along the $x$-axis, where it has a lobe width of one bin and an arbitrary lobe separation, a sticklet undergoes a smoothing process as it moves vertically up in the sticklet space. While retaining the starting lobe separation, a sticklet lobe gets wider until it reaches the diagonal where it becomes a Haar wavelet with equal lobe width and separation. In the remainder of the sticklet space, one encounters a combination of independently varied lobe widths and separations. Note that since one cannot have a sticklet with a lobe width wider than the separation without overlapping lobes, the sticklet space is confined to the triangular region below the Haar wavelet diagonal.

The primary advantage of the sticklet transform operator over the Haar wavelet is that it provides an additional degree of freedom in that we can change a sticklet's lobe width and separation independently, whereas the lobe width and separation vary together as we scale a Haar wavelet. We will show in what follows that this extra degree of freedom plays a key role in feature extraction utilizing sticklets.

Transform properties of the sticklet operator are illustrated in Figure 2. We operate with derivative, Haar wavelet and sticklet operators on a signal which contains both broadband and narrowband features. A derivative operator attenuates the broadband feature without affecting the narrow feature in the signal, while the Haar wavelet attenuates the sharp feature while preserving the broad feature. By contrast, the pure sticklet operator

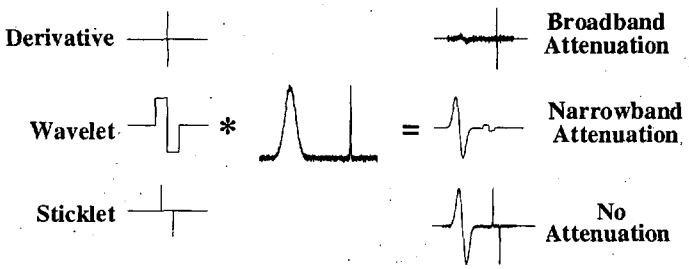


Figure 2. Attenuation signal features due to derivative, Haar wavelet and sticklet operators. Sticklet preserves both broadband and narrowband features in the signal.

preserves both the broadband and narrowband features of the signal; sticklets are able to detect desired signal features without attenuating features at different scales.

As shown in the earlier study[5], a sticklet operator can be constructed by combining (convolving) a derivative operator with a simple smoothing waveform. A derivative operating on a rectangular smoothing waveform yields a narrow sticklet with two single-bin lobes and a separation equal to the width of the rectangular waveform, while a triangular smoothing waveform leads to a Haar wavelet. A general sticklet with arbitrary lobe width and separation is a convolution of a derivative operator and a trapezoidal smoothing waveform.

We can define higher-order sticklets that have more lobes, with equal widths and same separations between lobes; the number of lobes in a higher-order sticklet is one more than its order. The even-order sticklets have reflection symmetry around a vertical axis, while the odd-order sticklets have diagonal reflection symmetry. For simplicity, the lobe amplitudes correspond to coefficients of Taylor's series expansion. Higher-order sticklets with narrow adjacent lobes of single-bin widths act as higher-order derivative operators.

## 3. FEATURE DETECTION AND ESTIMATION

A common approach to multivariate feature detection and estimation is the Classical Least Squares (*CLS*) method, a maximum likelihood estimator. With this method the *rms* error between the composite signal and a function composed of a set of candidate components, appropriately weighted by their strengths, is minimized. The composite signal in the matrix form is given by

$$S = K \cdot CL \ , \tag{1}$$

where the signal vector $S$ (length $n$, say) is related to component strengths given by vector $CL$ (length $m$, say) through a transfer matrix $K$ (dimensioned $n \times m$). The $K$ matrix contains the reference or library components, whereas vector $CL$ specifies their weights. Equation (1) describes how the composite signal $S$ is constructed from library components $K$ with the strengths specified by $CL$.

The component strengths can be estimated[11] by

$$CL = (K^T \cdot K)^{-1} \cdot K^T \cdot S \ , \tag{2}$$

where superscript $T$ signifies a matrix transpose and superscript $-1$ indicates the inverse of a matrix. In practice, one is given a composite signal $S$ with the task of estimating the strengths $CL$ of target components using eq. (2), given access to a library matrix $K$ of target components. As mentioned above, the *CLS* method often yields inaccurate and non-robust predictions since it is sensitive to any contributors to the composite signal that are not sought or accounted for, including non-random and random noise, and interferents similar to target components.

The Sticklet Least Squares (*SLS*) method involves an additional step before applying the maximum likelihood estimation: instead of using the given composite signal and library components, we utilize their sticklet transforms. Sticklet transforms are computed by convolving the composite signal and individual reference components with a response function representing an appropriate sticklet. Then, using these sticklet transforms, the component strengths are estimated with the *CLS* method as before. For each sticklet, characterized by its order, lobe width and lobe separation, the *SLS* method calculates a strength estimate for each target component.

Since both the lobe width and lobe separation can be adjusted independently in a sticklet of a given order, we can generate a two-dimensional (*2-D*) map of strength estimates for each target component as a function of sticklet width and separation. (The *2-D* strength estimate map discussed here is not to be confused with the wavelet transform of a signal or a *2-D* sticklet transform, not discussed here.) Following the convention of the sticklet space in Figure 1, strength estimates are plotted as a contour map with sticklet width along the *y*-axis and lobe separation along the *x*-axis. Such a *2-D* map displays at a glance which regions of the sticklet space (lobe width and separation) may offer superior predictions of the strength of a particular target component. It is important to realize that the *SLS* method generates an independent estimate map for each target component.

As we do not know *a priori* which sticklets offer good performance for a target component, we analyze a composite signal with known strengths of target components. From the *2-D* estimate map for each target component, we then select the sticklets that make the best predictions of its strength. In order to provide reliable and consistent predictions, these sticklets must be immune to the effects of varying non-random and random noise, and interferents. Once the component-specific sticklets are identified, we can apply them to any composite signal to yield accurate and robust estimates of target component strengths.

## 4. REMOTE CHEMICAL SENSING

In order to demonstrate the utility of sticklets in feature detection and estimation, we undertake the study of a fairly complex experimental scenario, as might be encountered in atmospheric remote sensing from an airborne platform. The objective is to estimate the concentrations of trace chemicals in the effluent plumes emanating from industrial smokestacks. We restrict our attention in this study to the daytime remote sensing scenarios in the mid-infrared spectral range (3 – 4 μm).

Solar radiation, reflected from an unknown background, propagates through the ambient atmosphere and through a localized plume under investigation, before reaching a remote sensor. We assume that the sole source of infrared radiation reaching the remote sensor is the reflected solar radiation, i.e. there are no emissions from the atmospheric or plume constituents. The spectral measurements are made by pointing the sensor in two viewing or look directions: through the plume under investigation and a nearby location outside the plume.

The on-plume composite spectrum measured at the sensor can be written as

$$I_{on} = R \cdot \rho \cdot T \cdot e^{-\sum \alpha_T} \cdot e^{-\sum \alpha_I} , \tag{3}$$

where $R$ represents the solar radiation spectrum impinging on the background, $\rho$ is the background reflectance, $T$ is the atmospheric transmission, $\sum \alpha_T$ represents the sum of absorption due to target chemicals in the plume, and $\sum \alpha_I$ represents additive absorption due to interferent chemicals in the plume. Note that all the quantities in eq. (3) are wavelength-dependent. Similarly, the off-plume composite spectrum can be written as

$$I_{off} = R' \cdot \rho' \cdot T' , \tag{4}$$

where the primed symbols represent the same quantities as in eq. (3); for the off-plume pointing direction, the absorption due both to target and plume interferent chemicals is absent. Since the incident solar radiation spectrum is the same in the nearby on-plume and off-plume look directions, we write the ratio of the on-plume and off-plume spectra as

$$R_I = I_{on} / I_{off} = (\rho / \rho')(T / T') e^{-\sum \alpha_T} e^{-\sum \alpha_I} . \tag{5}$$

Assuming that the background reflectance and atmospheric transmission are similar for the on-plume and off-plume look directions, we can write the composite signal as

$$S = \log_e R_I = \log_e(\delta\rho \cdot \delta T) + \sum \alpha_T + \sum \alpha_I + N \ , \qquad (6)$$

where $\delta\rho \equiv \rho / \rho'$ and $\delta T \equiv T / T'$ represent small fluctuations (around 1) between the on-plume and off-plume values of background reflectance and atmospheric transmission, respectively. We have added zero-mean Gaussian random noise, *N*, to the composite spectrum. Again, all quantities in eq. (6) are wavelength-dependent.

Our goal is to accurately determine the values of absorbance $\alpha_T$ (expressed as the product of volumetric concentration and path length or ppm-m) for target chemicals in the plume under investigation. This must be accomplished in the presence of unknown fluctuations in background reflectance ($\delta\rho$) and atmospheric transmission ($\delta T$), and against absorption $\alpha_I$ due to interferent chemicals in the plume and random noise *N*. We apply the two least squares methods to estimate $\alpha_T$, given the composite spectrum *S*.

## 5. BASELINE SCENARIO

We utilize a passive sensor in the mid-infrared spectral range, between wavenumbers 2880 $cm^{-1}$ (3.47 μm) and 3000 $cm^{-1}$ (3.33 μm). The library spectra for the target chemical species are measured in 2048 spectral bins separated by ~0.06 $cm^{-1}$. We also obtain spectra of background reflectance and random noise in the same spectral bins. For convenience in this proof-of-concept study, we generate the composite spectrum by adding absorbance due to specified concentrations of target chemicals to background reflectance contribution and random noise.

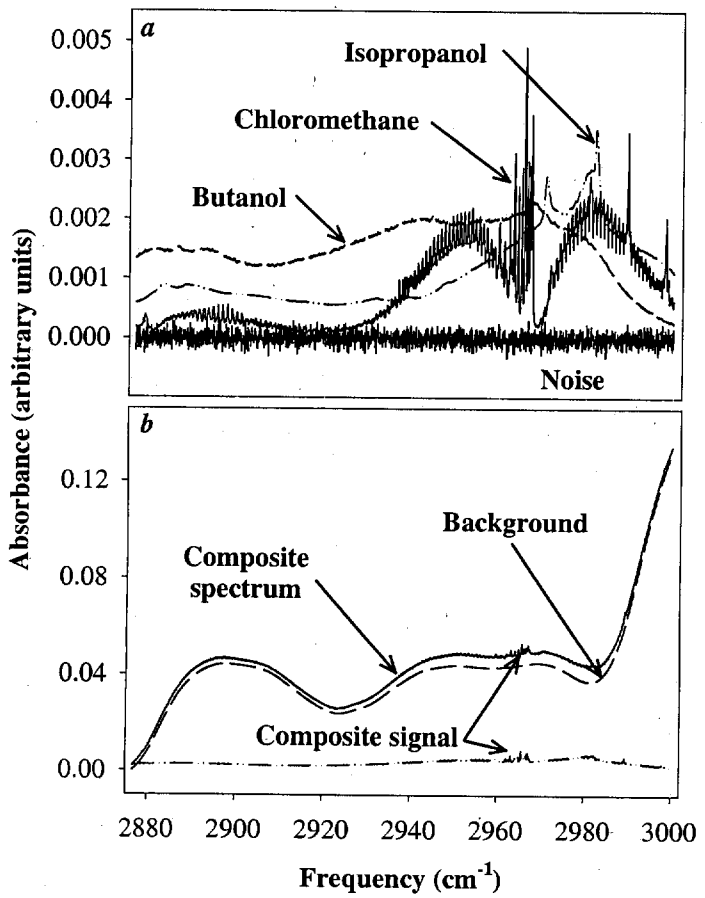


Figure 3. Clutter-dominated chemical environment. a. Mid-IR spectra of target chemicals. b. Clutter background and composite spectra. Clutter is about 20 times stronger than individual target absorbance.

The baseline chemical sensing scenario under study is shown in Figure 3. The spectra (absorbance vs. frequency) for three target chemicals - butanol, chloromethane (methyl chloride) and isopropanol - are shown in Figure 3a; a representative random noise spectrum is also shown. These molecules were chosen to represent narrow, medium and broadband spectral features: chloromethane has a large number of narrow spectral features, whereas isopropanol has two medium-width spectral features between 2960 and 2980 $cm^{-1}$. By comparison, the butanol spectrum lacks distinct features in the spectral range under consideration here.

We have chosen the concentrations of target chemicals (in ppm-m) to yield similar levels of absorbance (~0.002) in the mid-IR spectral region. The random noise is set at a level (~0.0001) that represents the instrument noise level approaching the theoretical limits for a 0.5 $cm^{-1}$ dispersive spectrometer on a sunny day[12].

We show the relative contributions of target chemical absorbance and background reflectance for the clutter-dominated

environment in Figure 3b; notice the different ordinate scale. The contribution of a representative material background, $\log_e \delta\rho$ (~0.04) from eq. (6), by far dominates the composite signal. For the baseline case, the random noise is a factor of ~400 below the background and the absorbance due to individual target chemicals is about 20 times the noise level (*SNR* ~20), i.e. a clutter-to-signal ratio of ~20.

As pointed out in the last section, the first step in the *SLS* method involves generating *2-D* estimate maps for the target chemicals since we do not know *a priori* which sticklets will yield accurate concentration estimates for each target chemical. Figure 4 presents examples of the concentration estimate maps for the three target

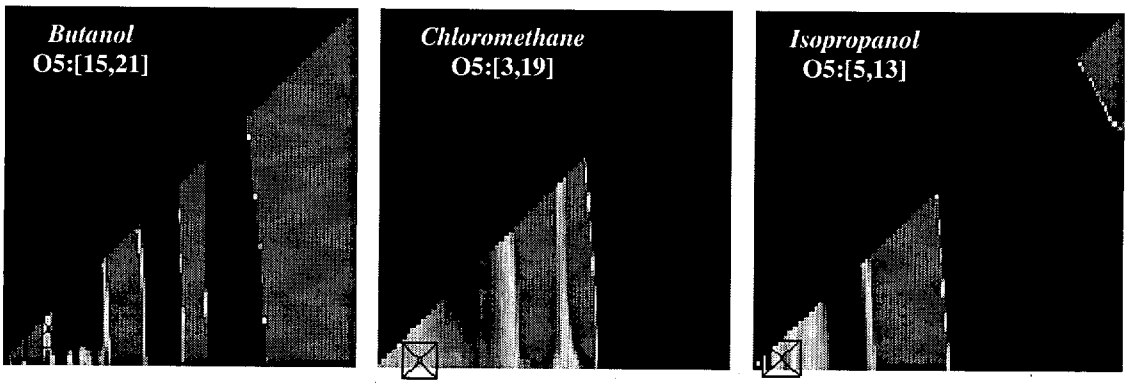


Figure 4. Concentration estimate maps for three target chemicals obtained with the sticklet least squares method. Sticklet lobe separation and width are along the *x*- and *y*-axis. Dark (grey) areas represent underestimates (overestimates) while light areas yield accurate predictions. Optimum sticklet marked for each target chemical.

chemicals generated with the *SLS* method. Recall that each *2-D* map follows the sticklet space convention in Figure 1 and displays the concentration estimate as a function of sticklet lobe width along the ordinate and lobe separation along the abscissa.

Each estimate map displays estimates within ±10% of the correct value, where dark (grey) areas indicate underestimates (overestimates) of more than 10%. Light regions of different size in the sticklet space yield good predictions for different chemicals. For butanol, limited number of sticklets offer superior performance, while chloromethane and isopropanol are characterized by extended areas of optimum sticklets. Sticklets yielding accurate predictions seem to be aligned in vertical bands, indicating that the lobe separation is a more important parameter than the lobe width.

Following a statistical procedure outlined in the previous study[5], we choose an optimum sticklet for each target chemical that yields a robust concentration estimate; optimum sticklets for the three chemicals under study here are shown in Figure 4. If one were to analyze an unknown composite spectrum using these molecule-specific optimum sticklets, one would expect to obtain accurate estimates of target chemical concentrations. Table 1 compares the concentration estimates obtained with the optimum sticklets with those using the *CLS*

**Table 1**
**Concentration Estimates**

| | *CLS* | *SLS* |
|---|---|---|
| Butanol (5 ppm-m) | 39.6 ± 0.01 ppm-m | O5:[15,21] 4.99 ± 1.3 ppm-m |
| Chloromethane (25 ppm-m) | 120.9 ± 0.09 ppm-m | O5:[3.19] 24.9 ± 0.16 ppm-m |
| Isopropanol (5 ppm-m) | 106.1 ± 0.02 ppm-m | O5:[5,13] 4.98 ± 0.07 ppm-m |

method. We also include in Table 1 an uncertainty in concentration estimates due to random noise realizations.

As mentioned earlier, in the presence of any contributors to the composite spectrum that are unknown or not accounted for, the *CLS* method can yield grossly inaccurate estimates. In Table 1, the *CLS* concentration estimates for the three target chemicals are inaccurate due to slowly varying clutter background included in the composite spectrum; the results are virtually insensitive to the high-frequency noise as seen by small uncertainty. By contrast, the *SLS* method yields very accurate predictions (error < 0.5%) that are subject to a somewhat larger imprecision due to random noise.

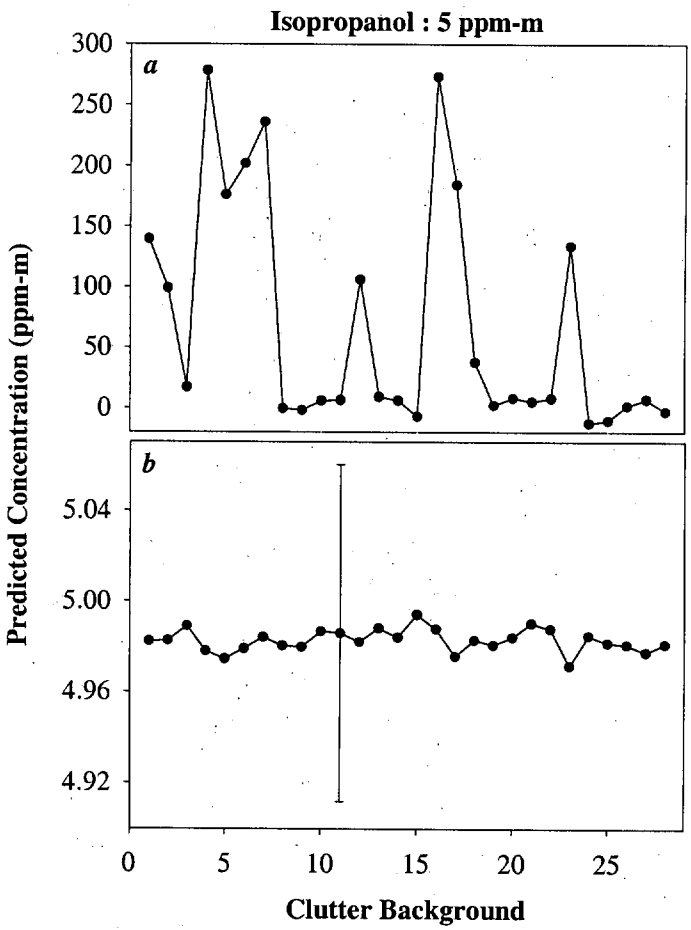


Figure 5. Clutter mitigation. Concentration estimates for isopropanol (5 ppm-m) with the *CLS* (a) and sticklet (b) methods. Error bars represent noise uncertainty in concentration estimates (too small to be seen in the *CLS* method).

To be useful, the optimum sticklet for each target chemical must provide robust concentration predictions against determinate noise such as background albedo and random noise, as well as interferent chemicals. In the previous study[5], we investigated in detail the impact of these factors, as well as varying clutter-to-signal and signal-to-noise regimes, on the performance of the sticklet transform method. For the remote chemical sensing scenarios we are considering here, background clutter is, by far, the most dominant contributor to the composite spectrum, as shown in Figure 4b; the contribution of atmospheric transmission will be discussed below. Although, the *CLS* method is insensitive to random noise, its predictions are strongly affected by slowly varying background reflectance.

Figure 5 compares the performance of the *CLS* and sticklet methods against different kinds of clutter backgrounds. The *CLS* prediction of isopropanol concentration varies widely (between –13 and 278 ppm-m) against different backgrounds, while the *SLS* method yields a very accurate (~4.99 ppm-m) which is virtually immune to varying clutter backgrounds. As pointed out earlier, the sticklet method is somewhat more sensitive to random noise as represented by the error bar in Figure 5b; the imprecision due to noise variations in the *CLS* method is imperceptible in Figure 5a.

Note that the *CLS* method can yield negative concentration estimates since it is an unconstrained maximum likelihood estimator; the *SLS* method, essentially the same least squares estimator preceded by a sticklet transform, can also yield negative concentration estimates, albeit far more infrequently.

## 6. EFFECT OF ATMOSPHERIC TRANSMISSION

Depending on the altitude and range of the remote sensor platform, reflected solar radiation, after passing through the effluent plume near ground, may propagate through a substantial extent of the atmosphere. If one includes atmospheric transmission, for example obtained from FASCOD3[13], in the analysis only through eq. 3, ignoring the off-plume signal, one ends up with a composite spectrum dominated by a large number of sharp absorption lines of atmospheric constituents, mostly water and methane in the mid-IR spectral band under study

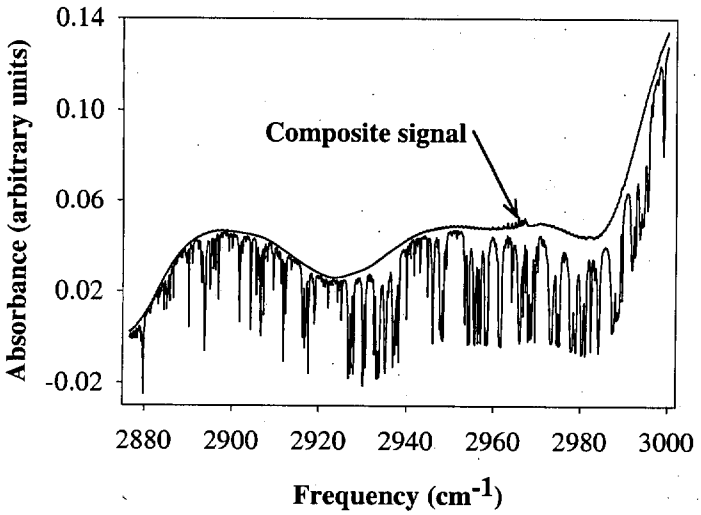


Figure 6. Composite spectrum (smooth curve) modulated by 5% differential atmospheric transmission (see text). Notice the composite signal (sum of absorbance due to trace amounts of three target chemicals) superimposed on the composite spectrum.

here. Under these circumstances, the sticklet method has little chance of success, particularly if atmospheric absorption lines attenuate the distinct spectral features of target chemical species.

The mitigating factor is the inclusion of the off-plume signal in the analysis. Considering that typical plume dimension is on the order of a few meters, especially upon emanating from the smokestack, the on-plume and off-plume look directions are separated by perhaps no more than 100 m. In such a circumstance, $\delta T = T/T'$ in eq. (6), representing small fluctuations in atmospheric transmission can be rewritten as differential transmission $\delta T \approx 1 - \varepsilon(1-T)$, where $\varepsilon$ is on the order of 1 – 10%. Then, one can include this differential transmission $\delta T$ with different values of $\varepsilon$ in eq. (6) for the composite spectrum.

We show in Figure 6 the composite spectrum modified by a 5% differential transmission, along with the original composite spectrum (smooth curve) from Figure 4b. Notice the composite target signal (sum of absorbance due to trace concentrations of three target chemicals), superimposed upon the smoothly varying clutter background; it is invisible in the presence of strongly-fluctuating atmospheric transmission.

It is not difficult to imagine that both least squares estimators would be hard-pressed to provide accurate or robust concentration predictions for the situation shown in Figure 6. Indeed, the *CLS* method offers concentration estimates that are not only grossly inaccurate but also change substantially as the level of differential transmission varies.

In order to assess the performance of the *SLS* method, we generate the *2-D* concentration estimate maps for three target chemicals for differential transmission levels of 1%, 2%, 5% and 10%. As an example, we show in Figure 7 estimate maps for isopropanol for the baseline case (no atmospheric transmission) and with 5% differential transmission. As before, light areas represent sticklets that provide accurate estimates; dark and grey areas provide underestimates and overestimates, respectively, beyond 50% of the true concentration of 5 ppm-m. Again, the lobe separation is along the abscissa and lobe width is along the ordinate.

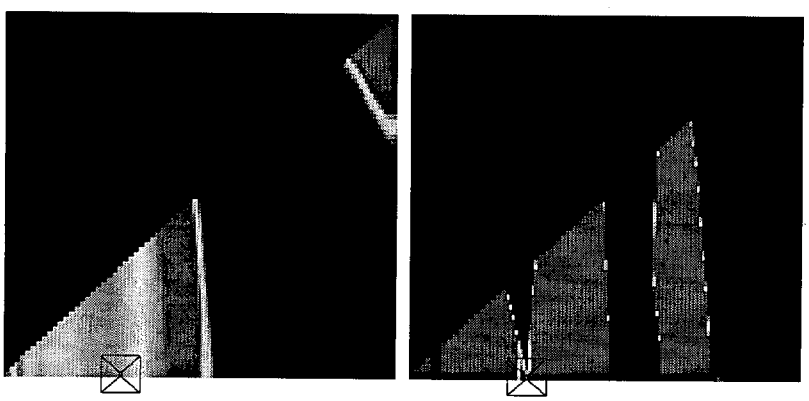

Figure 7. Concentration estimate maps for isopropanol (5 ppm-m). No atmospheric transmission included (left panel) and 5% differential transmission (right). Optimum sticklet O5:[1,45], marked on both panels, predicts isopropanol concentration within ± 10% error for differential transmission as high as 20%.

One immediately observes that in the presence of atmospheric transmission, there is a much smaller number of optimum sticklets that give satisfactory performance. Instead of extended light areas representing optimum sticklets (left panel of Figure

7), there are fewer optimum sticklets when atmospheric transmission is included in the analysis. Out of a total of some 10,600 sticklets encompassing the sticklet space, about 1400 give concentration estimates with an error of less than ± 10% in the absence of atmospheric transmission. By contrast, for the 5% differential transmission (right panel of Figure 7), there are only 20 optimum sticklets yielding estimates within ± 10% of the true concentration. Furthermore, upon combining the estimate maps with differential transmission up to 10%, we find that only 5 sticklets yield estimates with less than ± 10% error.

Table 2 lists these optimum sticklets and their predictions (average values and errors due to different levels of differential transmission). Optimum sticklet O5:[13,46] makes a very accurate but somewhat imprecise prediction, while a neighboring sticklet, O5:[15,46] offers a very precise, and slightly inaccurate, concentration estimate, against changing levels of differential transmission.

**Table 2**
**Optimum sticklets in the presence of differential atmospheric transmission**

| Isopropanol (5 ppm-m) | | Chloromethane (25 ppm-m) | |
|---|---|---|---|
| O5:[1,45] | 4.98 ± 0.32 ppm-m | O5:[1,92] | 24.5 ± 0.6 ppm-m |
| O5:[3,45] | 4.65 ± 0.07 ppm-m | O5:[3,92] | 25 ± 0.4 ppm-m |
| O5:[11,43] | 4.65 ± 0.06 ppm-m | O5:[5,36] | 24.8 ± 0.8 ppm-m |
| O5:[13,46] | 5 ± 0.23 ppm-m | O5:[7,75] | 27.1 ± 0.7 ppm-m |
| O5:[15,46] | 4.83 ± 0.01 ppm-m | O5:[9,28] | 25 ± 1 ppm-m |

A similar analysis of chloromethane estimate maps yields only 5 optimum sticklets that give estimates with less than ± 10% error; predictions of these optimum sticklets against differential transmission are also listed in Table 2. Using optimum sticklet O5:[3,92], one obtains an accurate and precise prediction for chloromethane concentration. It turns out that for butanol we find no optimum sticklets that give estimates within ± 50% error and that are robust against all levels of differential transmission up to 10%.

Another consideration is the atmospheric variability. The analysis so far has been done using a particular FASCOD3 atmospheric transmission model that has 25% relative humidity. Now we vary the relative humidity in our model from 10% to 40%. For isopropanol (true concentration of 5 ppm-m), the optimum sticklet O5:[13,46] predicts a concentration of 2 to 6.9 ppm-m against relative humidity rising from 10% to 40%. Optimum sticklet O5:[7,75] for chloromethane (25 ppm-m) yields 52 to 27 ppm-m for the same range in relative humidity.

In the original study[5], the optimum sticklets, obtained following a statistical analysis with random noise realizations, had the property that some of their lobes were aligned with distinct spectral features of the target chemical. This observation led to the idea of a specific set of "designer" sticklets for each target chemical that yields superior performance. For example, isopropanol has two features in the spectral range 2960 to 2980 $cm^{-1}$ with a separation of 11.3 $cm^{-1}$ (see Figure 4a). Notice that the lobe separation of optimum sticklets for isopropanol in Table 2 is between 43 and 46 bins (~2.82 $cm^{-1}$), i.e. approximately $1/4^{th}$ the separation between spectral features.

In Figure 8a-c, we show the composite spectrum (with 5% differential transmission), the library spectrum of isopropanol and the response function for optimum sticklet O5:[13,46], in the 2960 – 3000 $cm^{-1}$ spectral range. We have aligned the sticklet response function (panel c), by arbitrary scaling and shifting, to the library (panel b) and composite (panel a) spectra; the alignment is indicated by vertical dashed lines. One notices that the lobe width of the optimum sticklet is comparable to the two spectral features of isopropanol. The lobe separation closely matches the spectral distance between these features; note that one does not expect to perfectly match the lobe separation to the spectral features of a target chemical in the presence of random noise and atmospheric transmission fluctuations.

The situation for chloromethane is shown in Figure 8d-f. Two of the lobes of optimum sticklet O5:[3,92] are aligned almost perfectly with two prominent features of chloromethane around 2967 and 2989.5 $cm^{-1}$; again, the sticklet lobe width is comparable to the narrow features of the target chemical. The estimates with other optimum sticklets for chloromethane, listed in Table 2, suggest that there may be other configurations of optimum sticklets where various sticklet lobes may be aligned with other spectral features. Notice that the optimum sticklets seem to be aligned with spectral features where atmospheric transmission coefficient is high.

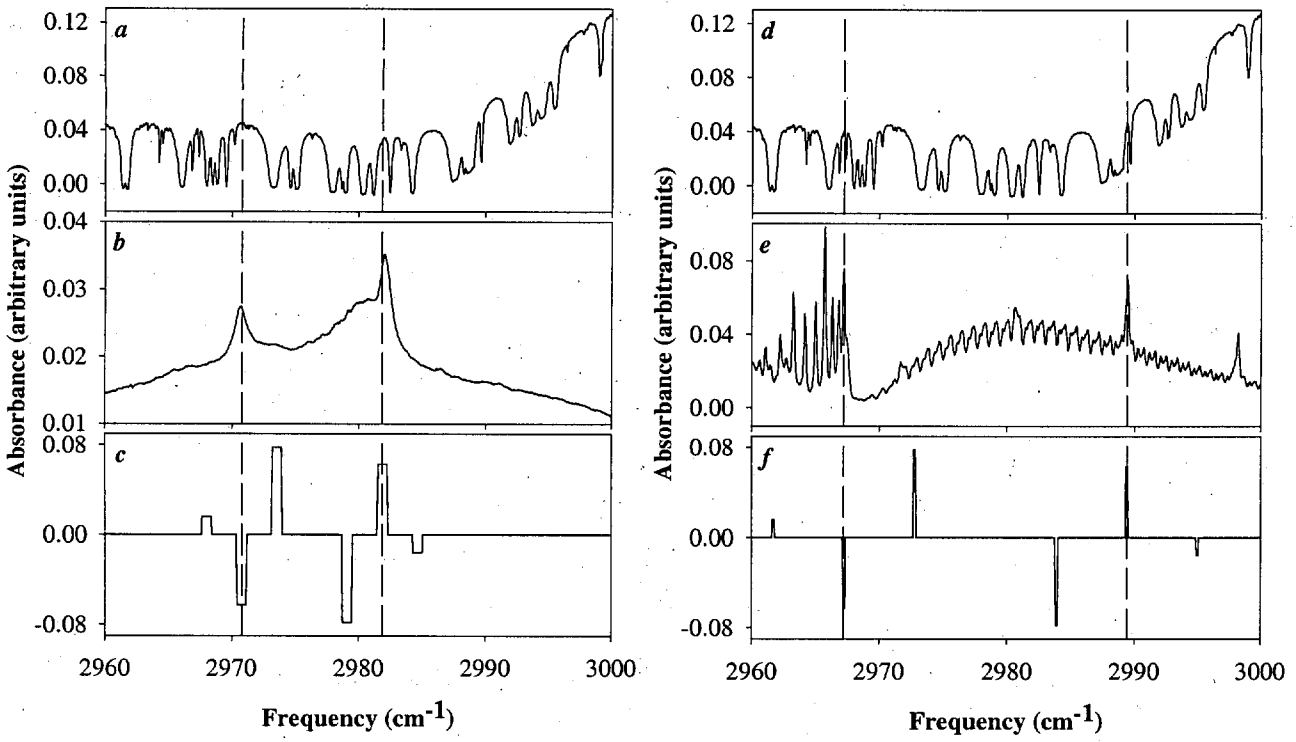


Figure 8. In the 2960 – 3000 $cm^{-1}$ spectral range, (a) composite spectrum with 5% differential transmission, (b) library spectrum of isopropanol (with two distinct spectral features) and (c) six lobes of the fifth-order optimum sticklet O5:[13,46]. Arbitrary scaling and shifting of sticklet for alignment with composite and library spectra, indicated by vertical dashed lines. (d-f) Same situation for chloromethane with optimum sticklet O5:[3,92].

## 7. CONCLUDING REMARKS

In a previous study[5], we demonstrated the utility of the sticklet transform method in robust estimation of trace chemicals in effluent plumes. The *SLS* method offers superior performance that is essentially immune to background clutter, and is largely insensitive to random noise and chemical interferents. In this report, we investigated the impact of including atmospheric transmission on the detection and quantitative estimation with the sticklet transform method in remote chemical sensing.

The differential nature of the sticklet transform makes it somewhat more susceptible to interferents with spectrally sharp features having significant absorption. This is the case with absorption by atmospheric constituents over the full atmospheric column. In order to ameliorate such effects, we examine remote sensing scenarios that look at the difference between the on-plume and off-plume measurements. This approach allows us to analyze data containing only a small fraction of the strong atmospheric attenuation in the mid-IR spectral range.

Computer simulations show that in the presence of varying levels of differential transmission up to 10%, we can find a set of optimum sticklets for isopropanol and chloromethane that give concentration estimates within $\pm$ 10% of the true values. For the spectrally broader molecule, butanol, we find sticklets that yield estimates within $\pm$ 50% of the true value up to differential transmission levels of 5%. This is to be compared to a fully saturated 1 meter water vapor plume that presents a 3.5% differential absorption. We anticipate further performance improvements by incorporating a model for the residual atmospheric absorption between on- and off-plume measurements. The largest contribution to the differential absorption is expected to be found near the ground level where the pressure-induced linewidths can be estimated to high accuracy. This should reduce the atmospheric residual to a much smaller value, providing even better sticklet estimates.

In agreement with the simulation results reported in the first study[5], we find that the optimum sticklets chosen by the *SLS* method are aligned closely with distinct and prominent spectral features of target chemicals, giving additional credence to the idea of a unique set of designer sticklets for each target chemical.

A number of issues remain to be resolved to complete the analysis of sticklets transforms in mitigating the effects of background clutter and atmospheric attenuation in remote chemical sensing. In particular, we plan to examine the performance impact of modeled residual atmosphere, as noted above, and of sensor effects such as spectral resolution, binning and instrument lineshape. Finally, a detailed comparison of the *SLS* method with other clutter mitigating schemes, such as principal component analysis[1], and with high quality remote sensing data, remains to be performed.

## ACKNOWLEDGEMENTS

We wish to thank Dr. Matt Pfenninger (LLNL) for fruitful discussions. This work was performed under the auspices of the U.S. Department of Energy by the University of California, Lawrence Livermore National Laboratory under contract W-7405-Eng-48.

## REFERENCES

1. A. Hayden, E. Niple and B. Boyce, "Determination of Trace-Gas Amounts in Plumes by the Use of Orthogonal Digital Filtering of Thermal-Emission Spectra," *Appl. Opt.*, **35**, 2802, 1996.
2. D. R. Morgan, "Spectral Absorption Pattern Detection and Estimation," *Appl. Spectrosc.*, **31**, 404, 1977.
3. D. Jouan-Rimbaud, B. Walczak, R. J. Poppi, O. E. de Noord and D. L. Massart, "Application of Wavelet Transform to Extract the Relevant Component from Spectral Data for Multivariate Calibration," *Anal. Chem.*, **69**, 4317, 1997.
4. J.-L. Starck, R. Siebenmorgen and R. Gredel, "Spectral Analysis using the Wavelet Transform," *Astrophys. J.*, **482**, 1011, 1997.
5. N. C. Mehta, E. T. Scharlemann and C. G. Stevens, "Sticklet: A Novel Transform Operator for Feature Detection and Estimation in Cluttered, Noisy Signals", to be submitted to *Applied Optics*.
6. J.-P. Kahane and P.-G. Lemaire-Rieusset, *Fourier Series and Wavelets* (Gordon and Breach, Philadelphia, PA, 1995).
7. G. Strang and T. Nguyen, *Wavelets and Filter Banks* (Wellesley-Cambridge Press, Wellesley, MA, 1996).
8. R. Raghuveer and A. S. Bopardiker, *Wavelet Transforms: Introduction to Theory and Applications* (Addison-Wesley, Menlo Park, CA, 1998).
9. J.-L. Starck, F. Murtagh and A. Bijaoui, *Image Processing and Data Analysis* (Cambridge University Press, New Yor, 1998).
10. S. Mallat, *Wavelet Tour of Signal Processing* (Academic, San Diego, CA, 1999).
11. R. Kramer, *Chemometric Techniques in Quantitative Analysis* (Marcel Dekker, New York, 1998).
12. C. Stevens, P. Kuzmenko and N. Thomas, "Cross-Dispersion Infrared Spectrometry (CDIRS) for Remote Chemical Sensing," *Proc. SPIE*, **2552**, 284, 1995.
13. S. A. Clough, F. X. Kneizys, G. P. Anderson, E. P. Shettle, J. H. Chetwynd and L. W. Abreu, "FASCOD3: Spectral Simulation," in *IRS '88: Current Problems in Atmospheric Radiation-Proceedings of the 1988 International Radiation Symposium*, ed., J. Lenoble and J.-F. Geleyn (Deepak Publishing, Hampton, VA, 1989).

University of California
Lawrence Livermore National Laboratory
Technical Information Department
Livermore, CA 94551